Low-altitude ion heating with downflowing and upflowing ions

Yangyang Shen[1], David J Knudsen[1], Johnathan K Burchill[1], Andrew Howarth[1], Andrew Yau[1], Gordon James[1], David M Miles[2], Leroy Cogger[1]

1.Department of Physics and Astronomy, University of Calgary, Calgary, AB, Canada

2. Department of Physics, University of Alberta, Edmonton, AB, Canada

1. Introduction

Mechanisms and their relative importance in driving O^+ ion heating and ion upflow in the topside ionosphere have not been fully resolved yet. The objectives of this study are:

- To test whether wave-ion heating contributes significantly to the ion energization process at 300 -700 km altitudes, where previous studies assume that frictional heating or Joule heating dominates.
- To create statistics of low-altitude ion heating and ion flow observations with wave and plasma measurements, since no statistics exists except sporadic sounding rocket observations.
- To study fine structures of and correlations between field-aligned flow velocity, ion heating and field-aligned currents (FACs) with up to 10-ms temporal resolution (~80 m spatial resolution) low-energy (<100 eV) ion measurements.

We use one-year recordings of simultaneous ion, magnetic field, wave electric field and optical data from the e-POP satellite for this study.

2. Methodology

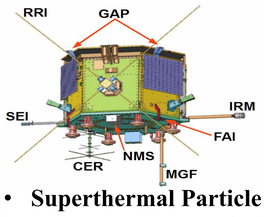

Figure 1. e-POP instruments on the CASSIOPE satellite operating since September 2013 in a nearly polar orbit (325-1500 km). Data obtained between March 2015 and March 2016 are used for this study.

- **Superthermal Particle Imager (SEI):** Vertical ion velocity and ion temperature are derived from 100-image-per-second low-energy 2-D ion distribution functions [*Knudsen et al. 2015*].

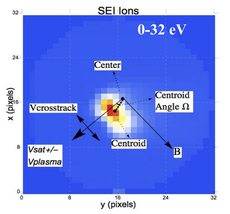

Figure 2. A typical SEI flight image.

The ion upflow velocity (along B) is:

$$V_{\parallel} = V_c \cdot \hat{b} = \left(V_s \pm V_p\right) \times \tan\Omega \cdot \hat{b} \simeq V_s \times \tan\Omega \cdot \hat{b}$$

The ion temperature data can be estimated by the width of the ion distribution function (FWHM) [*Shen et al. 2016*].

- **Ion Mass Spectrometer (IRM):** 100-image-per-second 2-D ion distribution functions and ion composition in the energy range 0-100 eV/q.
- **Radio Receiver Instrument (RRI):** up to 30 kHz radio wave electric fields (10 Hz –18 MHz dynamic range available).
- **Fluxgate Magnetometer (MGF):** 160 Hz vector magnetic field.
- **Fast Auroral Imager (FAI):** large-scale auroral emissions.

3. Results

Example 1: Nightside Aurora

Kp: 5+ Altitude: 410km MLAT: -73.2º MLT 1.6h O+ dominates

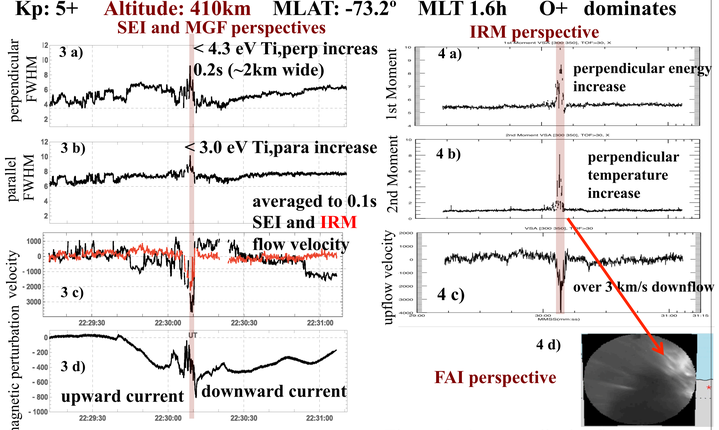

Figure 3. a) perpendicular-to-B FWHM time series. b) parallel-to-B FWHM time series. c) ion upflow velocity profile. d) magnetic field east perpurbations with positive slope representing downward FACs.

Figure 4. a) perpendicular first moments from IRM representing average energy. b) 2nd Moment profile indicating ion temperature. c) ion upflow velocity. e) FAI auroral rays in the heating region.

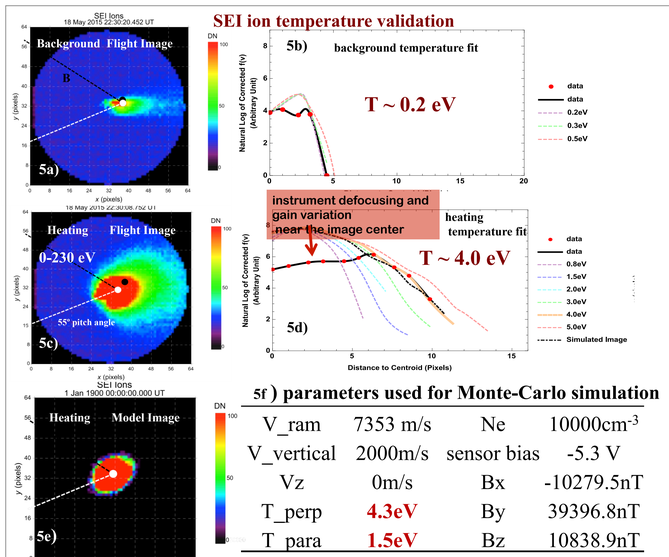

V_ram	7353 m/s	Ne	10000cm^{-3}
V_vertical	2000m/s	sensor bias	-5.3 V
Vz	0m/s	Bx	-10279.5nT
T_perp	**4.3eV**	By	39396.8nT
T_para	**1.5eV**	Bz	10838.9nT

Figure 5. Flight images (integrated to 10 images per second) simulated using a Monte-Carlo charged particle ray tracing tool adapted to the SEI instrument. The slopes of the ion distribution functions at 55º pitch angle are fitted with different Maxwellian temperatures. Panels 5a&5b display the quiet time background image with the slope fit indicating 0.2 eV background ion temperature. Panels 5c&5d show the most intense heated image and slope fit result. Panel 5e displays the simulation image with the parameters shown in 5f. The calibrated parallel ion temperature is 1.5 eV instead of 3.0 eV from Figure 3b.

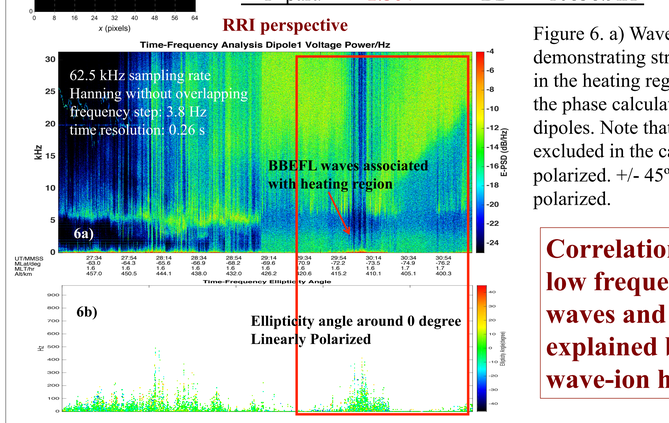

Figure 6. a) Wave electric fields (0-30 kHz) spectrogram, demonstrating strong emissions below 500 Hz (BBELF) in the heating region. b) Ellipticity angle distribution from the phase calculation of electric fields from RRI cross dipoles. Note that small PSD wave emissions have been excluded in the calculation. 0º indicates purely linearly polarized. +/- 45º is left-hand (right-hand) circularly polarized.

Correlation with broadband extremely low frequency (up to 3 kHz, BBELF) waves and $T_\perp$ increase that cannot be explained by frictional heating suggest wave-ion heating!

Example 2: Dayside Cleft

Kp: 2- Altitude: 357 km MLAT: -77º MLT 15.2h IMF By>0

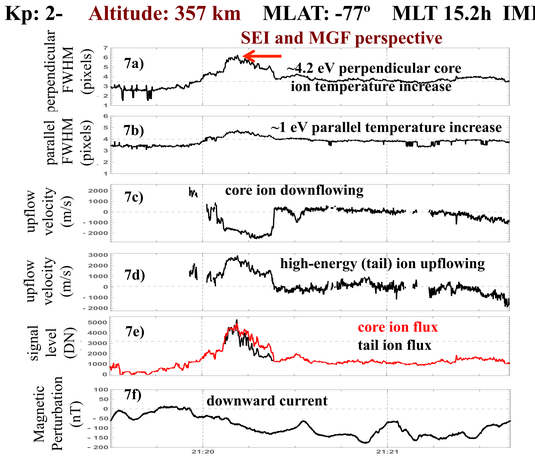

Figure 7. a) perpendicular-to-B FWHM time series. b) parallel-to-B FWHM time series. c) core ion (red pixels in Figure 8b) field-aligned flow velocity profile. d) tail (high-energy) ion field-aligned flow velocity profile. e) comparison between core ion flux (red) and tail ion flux (black). f) magnetic field east perturbations with negative slopes representing downward FACs.

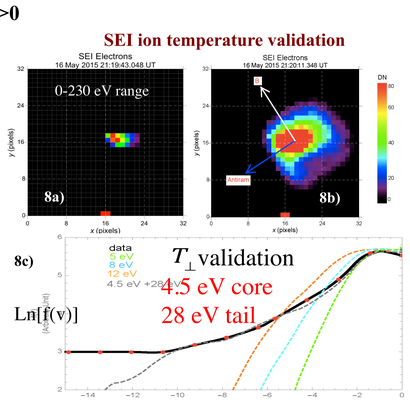

Figure 8. Background (8a) and heated (8b) flight images and perpendicular-to-B temperature calibration (8c), indicating about 4.5 eV core ion heating with 28 eV tail heating. Note that in 8b, there is a confined high-energy ion population going downward the field line.

Statistics: 24 clear ion heating events

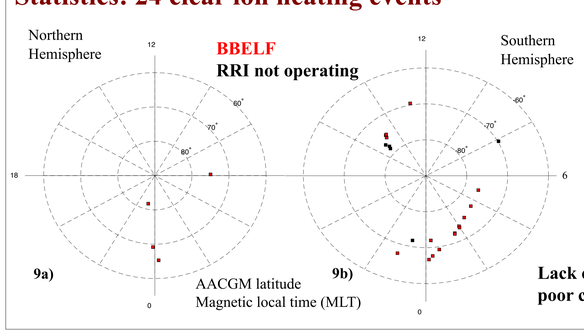

at least 18 out of 24 ion heating events have BBELF waves!

Figure 9. AACGM latitude and MLT distribution of the 24 ion heating events. Majority of these events are located at nightside auroral region in the southern hemisphere.

Lack of dayside cleft events is due to poor coverage of measurements.

heating	Date_StartTime_EndTime	Ion flow	Wave?	Aurora?	Altitudes(km)	Kp
1	20150518_222913_223111	down	BBELF	FAI	412	5+
3	20150518_205400_205543	up and down	BBELF		351, 351, 351	3 to 5+
1	20150516_211930_212140	down(up)			358	2-
1	20150517_210645_210916	up			357, 355	0+
3	20150608_125300_125712	down	BBELF	FAI	400,400, 440	4+
1	20150609_124147_124312	down	BBELF	FAI	434	3
1	20150612_115914_120412	down	BBELF	FAI	441	2+
1	20150613_114514_115112	down	BBELF	FAI	469	2+
3	20150616_110614_111000	down	BBELF	FAI	461, 469, 483	2-
1	20150623_093625_094119	down		FAI	708	5+
1	20151110_061644_062010	down and up	BBELF	FAI	413	5
2	20151119_054220_054712	up	BBELF	FAI	335, 339	2-
1	20151005_141800_142218	up	BBELF		443.8	3
1	20160301_232235_232545	down	BBELF		730	3-
1	20150909_085230_085647	up and down		FAI	386	6
1	20150919_075900_080500	down			423	5-
1	20150911_082400_082600	up and down		FAI	360	7

Table 1. Summary of all the heating events with indication of orbit time, the field-aligned flow pattern, association with BBELF, aurora appearance, altitude, and Kp level.

17 out of 24 ion heating events have ion bulk downflow!

Correlation of ion heating with ion downflow: Excerpts

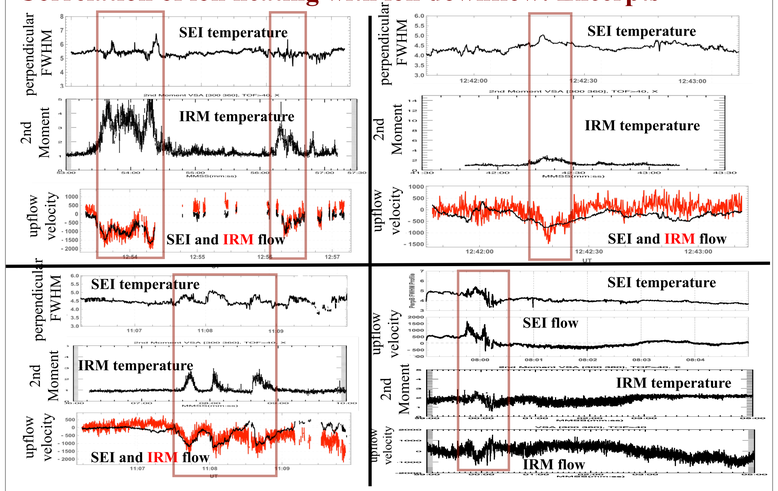

Figure 10. Excerpts from four cases showing correlation between perpendicular ion temperature increase and ion downflow observed by SEI and IRM.

4. Conclusions

1. 24 low-energy ion heating events from several different instruments provide convincing statistics and complementary views of the low-altitude ion energization process and its relation with field-aligned flows and FACs.
2. Transverse ion heating can be intense (up to 4.5 eV), very narrow (~2 km across B), is more likely in the downward current region, and is associated with BBELF waves between 330-730 km altitudes. This suggests that significant wave-ion heating should be included in relevant models at low altitudes.
3. The minimum altitude of strong wave-ion heating (~350 km) is lower than reported in the literature [*Whalen et al. 1978*].
4. Contrary to what would be expected from mirror-force acceleration of heated ions, the majority of these heating events (17 out of 24) are associated with core ion downflow rather than upflow. Unknown processes are involved.

5. References

[1] Knudsen, D., J. Burchill, T. Cameron, G. Enno, A. Howarth, and A. Yau (2015), The CASSIOPE/e-POP Suprathermal Electron Imager (SEI), Space Science Reviews, 189(1-4), 65-78, doi:10.1007/s11214-015-0151-1.

[2] Shen, Y., D. Knudsen, J. Burchill, A. Howarth, A. Yau, R. Redmon, D. Miles, R. Varney, and M. Nicolls(2016), Strong ambipolar-driven ion upflow within the cleft ion fountain during low geomagnetic activity, J. Geophys. Res. Space Physics, 121, 6950–6969, doi:10.1002/2016JA022532.

[3] Whalen, B. A., Bernstein, W. and Daly, P. W. (1978), Low altitude acceleration of ionospheric ions. Geophys. Res. Lett., 5: 55–58. doi:10.1029/GL005i001p00055.

6. Acknowledgement

This work is supported by a Eyes High Doctoral Recruitment Scholarship from University of Calgary and the Natural Sciences and Engineering Council of Canada. e-POP is funded by the Canadian Space Agency. We thank Gareth Perry for assistance with RRI data and helpful discussion.

Email: *yangyang.shen@ucalgary.ca*

Poster Number : MITC-08